LUND UNIVERSITY

Design of bezel antennas for multiband MIMO terminals using characteristic modes

Miers, Zachary; Li, Hui; Lau, Buon Kiong

Published in:
European Conference on Antennas and Propagation (EuCAP), 2014

DOI:
10.1109/EuCAP.2014.6902342

2014

Document Version:
Peer reviewed version (aka post-print)

Link to publication

Citation for published version (APA):
Miers, Z., Li, H., & Lau, B. K. (2014). Design of bezel antennas for multiband MIMO terminals using characteristic modes. In *European Conference on Antennas and Propagation (EuCAP), 2014* (pp. 2556-2560). IEEE - Institute of Electrical and Electronics Engineers Inc.. https://doi.org/10.1109/EuCAP.2014.6902342

Total number of authors:
3

LUND UNIVERSITY

PO Box 117
221 00 Lund
+46 46-222 00 00

Design of Bezel Antennas for Multiband MIMO Terminals Using Characteristic Modes

Zachary Miers, Hui Li, Buon Kiong Lau
Department of Electrical and Information Technology, Lund University, Lund, Sweden, Zachary.Miers@eit.lth.se

***Abstract*—Designing decorrelated MIMO antennas in small mobile terminals at frequencies below 1 GHz is challenging since more than one antenna tend to excite the single resonant mode available to a typical chassis structure. This challenge increases even further when multiple frequency bands are required from each antenna. Recently, a design framework to obtain efficient and decorrelated MIMO antennas based on the Theory of Characteristic Modes was proposed. By slightly modifying the chassis, multiple orthogonal resonant modes may be created and excited to facilitate low correlation at frequencies below 1 GHz. In addition, multiband operation per antenna can be achieved by correlating the characteristic currents of different modes across different frequency bands. In this work, we apply the proposed framework to make opportunistic use of the bezel structure popular in mobile terminal designs to achieve efficient and uncorrelated multiband MIMO antennas.**

***Index Terms*— Antenna array, antenna design, characteristic modes, MIMO systems, mutual coupling, mobile antenna.**

I. Introduction

The challenge of terminal antenna design has dramatically increased due to the wide adoption of multiple-input multiple-output (MIMO) technologies. This is because it is difficult for multiple antenna elements that are packed into an electrically small volume to support good MIMO performance, due to their proximity to one another. Moreover, at frequencies lower than 1 GHz, these antennas typically rely on the common chassis (ground plane) to obtain larger bandwidth and radiate more efficiently, resulting in strong mutual coupling and correlation between the elements [1].

Even though numerous techniques have been proposed in the literature to mitigate coupling between antenna elements [1], relatively little attention has been given to the problem of chassis induced coupling. Recent studies reveal that the Theory of Characteristic Modes (TCM) [2] can be employed to effectively mitigate chassis induced coupling. In effect, the fundamental radiation properties of the chassis as obtained from the TCM facilitate the selection of the appropriate location [3] and/or radiation properties [4], [5] of the antenna elements on the chassis. However, the common principle of these strategies is to only allow one antenna to exploit the chassis as a radiator, which means that other antennas may suffer in terms of bandwidth performance.

More recently, based on analysis using the TCM, minor modifications of the chassis structure has been proposed to support multiple decoupled modes below 1 GHz [6], [7]. Follow-up work in [8] took this further and proposed the technique of correlating characteristic currents across frequencies to improve bandwidth and enable multiband operation. As proof of concept, a dual-band (818-896 MHz, 1841-2067 MHz), dual-antenna prototype was designed on a 130 mm × 66 mm chassis for LTE operation. The design in [8] is based on the addition of metallic strips along the two longer sides of the chassis.

In this work, we further substantiate the flexibility of the design methodology of [8] by applying it to a terminal chassis loaded with a metallic bezel. The bezel ("side wall") is a popular design feature in recent mobile terminals and has the advantages of being mechanically strong, easy to manufacture, and aesthetically pleasing. Using the method of [8], a dual-band dual-antenna design with low correlation and high efficiency can be achieved on a chassis loaded by a metallic bezel.

II. Low Frequency Modal Formation

The design framework presented in [8] is applied here to a mobile phone chassis with dimensions 130 mm × 66 mm × 8 mm (see Fig. 2). This structure was analyzed using the TCM [2], with the eigenvalues at low frequency bands shown in Fig. 1. The eigenvalue of each characteristic mode directly corresponds with the imaginary component of the characteristic impedance; when the eigenvalue is zero, the mode is resonant. As can be seen, the bezel structure supports three resonant eigenmodes below 1 GHz. No two modes below 1 GHz can be simultaneously excited at any frequency with sufficient bandwidth.

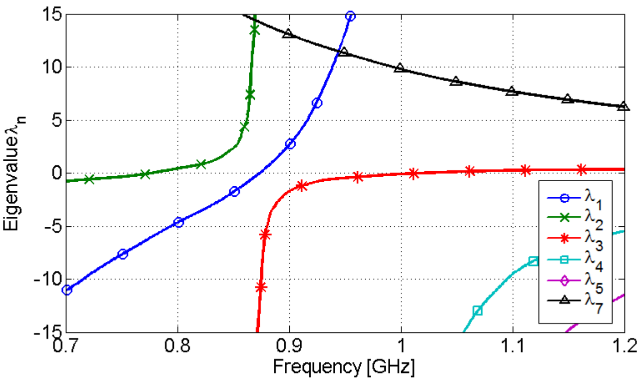

Fig. 1. Characteristic eigenvalues over frequency for a 130 mm × 66 mm chassis with an 8 mm bezel wrapped around the exterior of the chassis.

This work was supported by Vetenskapsrådet under grants no. 2010-468 and 2012-4859.

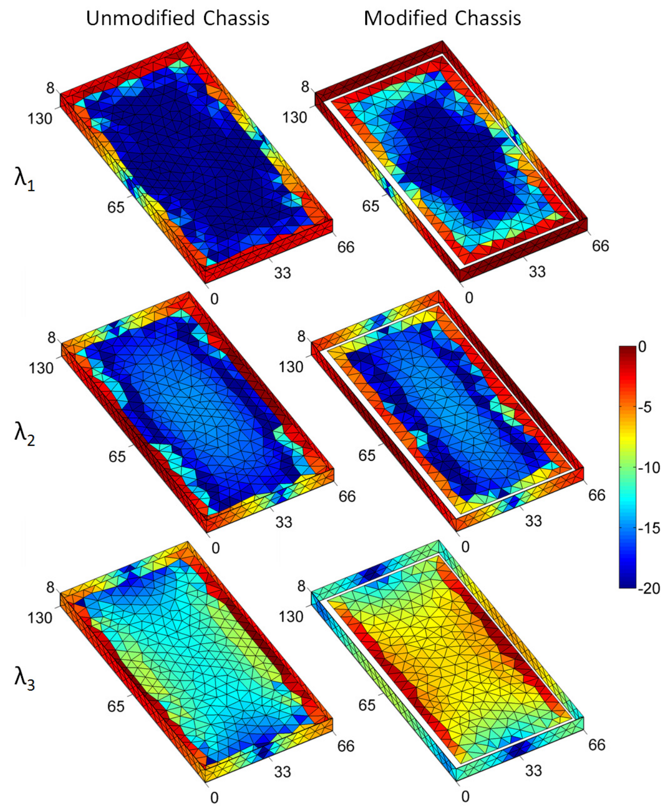

Fig. 2. The modal currents of λ_1, λ_2, and λ_3 of the unmodified and modified chassis at 800MHz.

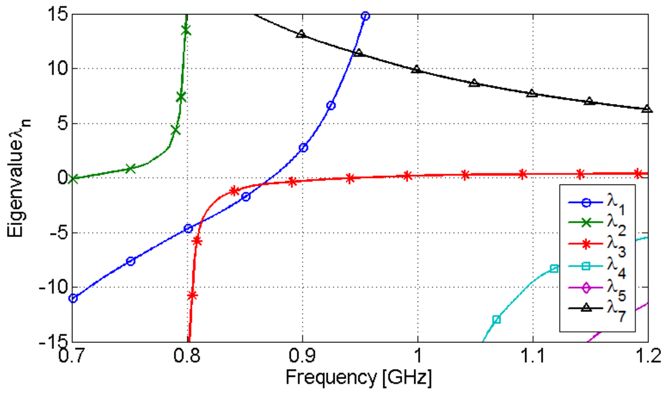

Fig. 3. Characteristic eigenvalues over frequency for the low frequency modified bezel with ground plane dimensions of 121 mm × 59 mm and bezel dimensions of 130 mm x 66 mm x 8 mm. The ground plane is shifted from the center of the bezel along the width by 4 mm.

λ_1 supports a current distribution matching that of a resonant loop antenna around the bezel and chassis. λ_2 supports current distributions along both longer edges of the chassis, creating a far field pattern resembling that of two dipole antennas separated by the width of the chassis. λ_3 supports the fundamental chassis mode with the current distribution of a thick flat dipole along the length of the chassis. Through correlating the currents in each of these modes, it is seen that the currents are highly coupled around the bezel but largely decoupled throughout the chassis, as is shown by the modal currents in Fig. 2. By means of adjusting the surface area of the flat conductive ground plane situated in the center of the bezel, a spacing (or gap) is formed between the ground plane and bezel; this causes λ_2 and λ_3 to shift uniformly in frequency. λ_1 shifts in frequency through moving the center position of the ground plane in reference to the center position of the bezel.

Through slight adjustments of the absolute size of the conductive ground plane and the absolute position of the ground plane in reference to the bezel, multiple excitable modes can be formed at frequencies below 1 GHz as shown in Fig. 3 at 850 MHz. Each of these modes can be independently fed by analyzing the modified characteristic currents (Fig. 2) and near-fields (Fig. 4) and applying the proper feeding element for each mode [9]. A capacitive coupling element is able to couple (or feed) power into the chassis if there is a significant characteristic electric field in the vicinity and direction of the element. In contrast, if electric field is not present (or weak) in the area around the feed, coupling between the element and the chassis is not possible. Through analyzing the electric fields of both λ_1 and λ_3 in Fig. 4, locations can be found where the electric field is at a minimum for one mode and a maximum for the other mode. By placing coupling elements at these locations, it is viable to feed the two modes individually with minimal coupling between the separate modes.

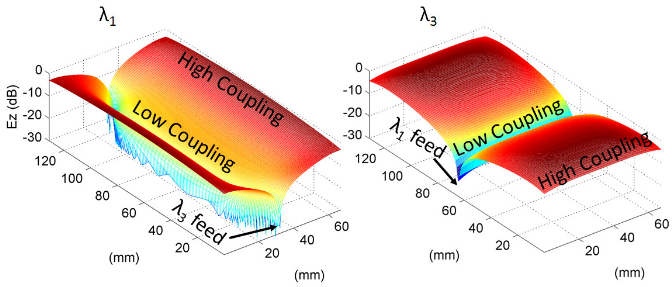

Fig. 4. The electric near fields in the z direction of the low frequency modified chassis at 850MHz.

In an effort to extend the bandwidth of one or more of the modes, λ_1, λ_2, and λ_3 were cross correlated with one another. The cross correlation analysis indicated high correlation between λ_2, and λ_3 along the top of the chassis in both the y and z components of the characteristic electric fields. Through the implementation of a capacitive coupling element which coupled energy into the chassis through y and z directed electric fields, chassis induced coupling could be exploited to excite both λ_2, and λ_3 through a single feed. However, due to the difference in their impedance values, a suitable matching network could not be found in which both modes could be excited using a single feed and thus low frequency bandwidth extension through multimode coupling was not possible without further chassis modification [8]. A second coupling element was attached to the bezel along the width of the chassis to induce z and x directed electric fields, which coupled into and excited λ_1. Both feeds utilized an L-matching network to match the port feed to the respective eigenmode.

III. MULTIBAND RESPONSE

It is possible to further manipulate the structure to support multiple resonances, based on the same low frequency feed locations. Through cross correlating the area around the feeds with the currents and near-fields of higher frequency modes, it was possible to determine what modifications to the chassis could produce uncorrelated resonances above 1 GHz. Ports 1 and 2 produced significant *z* directed electric fields at frequencies above 1.5 GHz, which coupled strongly to λ_1, λ_5, and λ_6 at their respective resonant frequencies (see Fig. 5). In the current form, the chassis did not allow for the two ports to independently excite any of the resonant modes at the low frequency feed locations without significant port-to-port coupling. To excite two independent modes of radiation, the structure had to be modified so that the *z* directed electric fields independently excite different modes of operation. Many different chassis modifications could be found to create additional modes. One simple modification is to insert a resonant feature or structure into the chassis which can be excited through electric field coupling. One such modification to the structure is to add a small half wavelength slot into the ground plane directly beneath the capacitive coupling element of port 1. Any coupling that passes through the slot will excite the slot and radiate energy. The addition of the slot into the side of the ground plane shifted the resonant frequency of λ_4 from 2.9 GHz to 1.85 GHz, as seen by λ_4 Modified in Fig. 5. This modification did not significantly influence the low frequency eigenmode resonances.

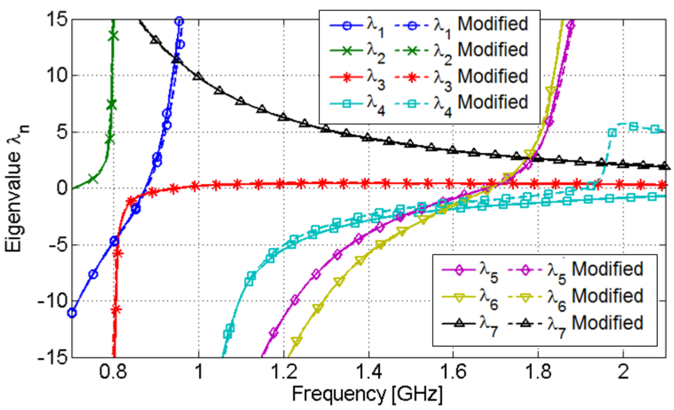

Fig. 5. Characteristic eigenvalues over frequency for a 121 mm × 59 mm ground plane with a 130 mm × 66 mm × 8 mm bezel. λ_3, λ_5, and λ_6 are excited by z directed electric fields in the locations of both port 1 and 2.

A near-field analysis of the dual band modified structure showed that in order to fully decouple the two ports from one another, as was done for the low frequency feeds, the slot should not be fed in the center of the structure but rather at a 10 mm offset along the length of the chassis. However, if the feed placement were to be moved, the low band excitations would couple to one another. To avoid significant high band coupling while maintaining high isolation in the low band, the electric fields of the coupling element must be well matched to the electric fields of resonant slot. This can be done through characteristic mode analysis of the slot within the chassis. Shifting the location of the slot in reference to the chassis rather than the feed in reference to the slot makes it possible to align the maximum of the slot mode electric field with the maximum electric field of the coupling element. The peak of the *z* and *x* directed electric fields for the slot antenna were shown to be 15 mm off center of the slot at 1.85 GHz. Placing the slot 15 mm away from the center of the chassis improved the bandwidth and port matching while decreasing the total coupling between port 1 (feeding λ_4) and port 2 (feeding λ_3) from a peak coupling of -5.5 dB at 1.9 GHz to a peak coupling of -9.1 dB at 1.99 GHz. The improved matching and isolation significantly increases the total efficiency. In addition, it was observed that the coupling between the two ports occurred primarily through coupling currents along the bezel, which had little impact on the radiation properties of the two orthogonal modes λ_3 and λ_4. This implies that the coupling has minimal impact on the envelope correlation coefficient (ECC).

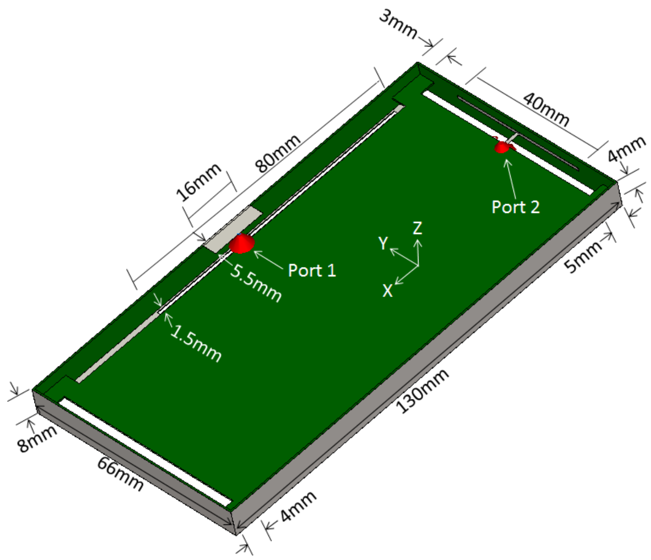

Fig. 6. Final design of a 130 mm × 66 mm × 8 mm bezel multi-antenna multi-band chassis.

In the current form, the structure can in fact support additional decoupled higher frequency modes for MIMO operation (e.g., at 2.6 GHz and 3.5 GHz). Though it is outside the scope of this paper, the same procedure as described in this section can be used to improve the impedance matching and decrease the coupling at the higher frequency bands.

IV. FULL-WAVE VERIFICATION

The proposed antenna system was implemented into a full wave model and simulated using the frequency domain solver of CST Microwave Studio. In an effort to use industry-acceptable materials and prototype this antenna in a cost-effective manner, the antenna was adapted for fabrication on a dielectric carrier. The dielectric material (with relative permittivity $\varepsilon_r = 2.95$ and loss tangent tan $\delta = 0.028$) loaded both the fundamental mode and the orthogonal mode, such that minor re-tuning of the structure was needed. Specifically, the length of the slot antenna was changed from 80 mm to 84 mm and the length of the ground plane was reduced by 1 mm to increase low band resonant frequency of the dipole mode. The final multi-band multi-antenna bezel chassis as was designed through characteristic mode analysis is shown in Fig. 6. The dimensions of the two capacitive coupling feed elements as well as the final dimensions and location of the slot were adjusted for maximum isolation. The high band excitations did not need external matching components to radiate efficiently. Moreover, the L-matching network used to match the low band of both ports acts as high pass filters and did not significantly impact the high band performance.

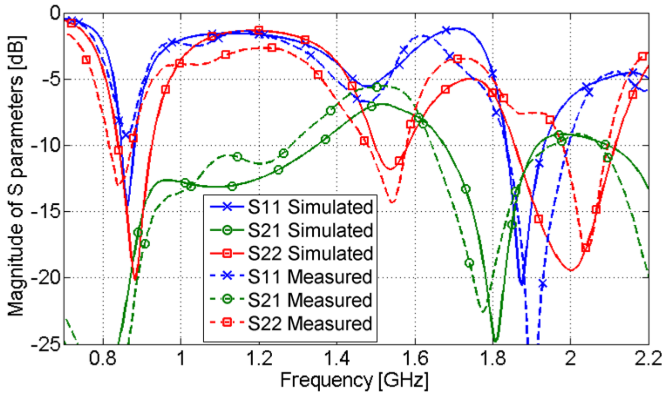

Fig. 7. CST simulated and measured S parameters of the proposed bezel chassis dual-antenna system.

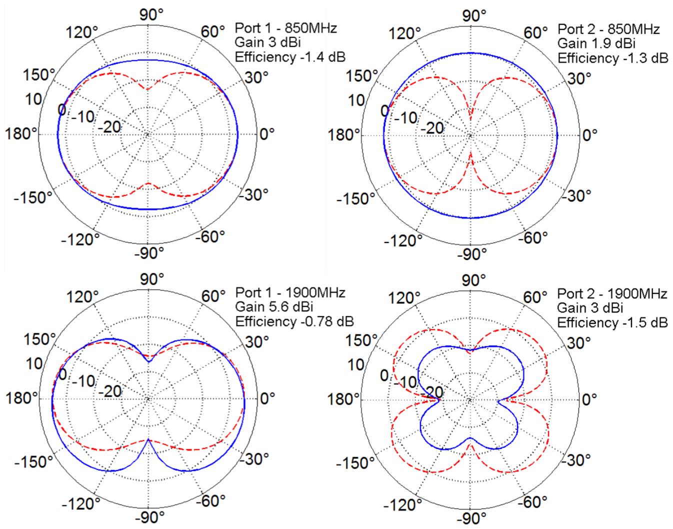

Fig. 8. CST simulated *y-z* (solid blue line) and *x-z* (dashed red line) principle plane patterns of port 1 and port 2.

The dimensions of the capacitive coupling elements of ports 1 and 2 were optimized to increase the total bandwidth of each port while maintaining high isolation between the two ports in both bands of operation. The L-matching networks utilized Murata lumped element components with port 1 consisting of a 3.9 pF series capacitor and a 7.5 nH parallel inductor, and port 2 consisting of a 1.8 pF capacitor and a 15 nH inductor. Port 1 produced a 6 dB match from 824 MHz to 896 MHz and from 1.8 GHz to 2.16 GHz, whereas port 2 was matched from 811 MHz to 960 MHz and from 1.81 GHz to 2.01 GHz (see Fig. 7). The average simulated ECC (calculated with uniform 3D angular power spectrum (APS)) for both bands was below 0.1, and the total efficiency was higher than -1.5 dB in both bands. The simulated 3D radiation patterns (see Fig. 8) closely match simulated characteristic patterns.

V. Prototype Verification

The proposed bezel antenna was fabricated directly from the CST full wave model. Microstrip feed lines and SMA connectors were added to the prototype for practical testing purposes (see Fig. 9). The measured scattering (S) parameters (i.e., the dashed lines in Fig. 7) correspond well with the simulated S parameters. The far-field patterns (see Fig. 10) and total efficiencies of the antennas were measured in an anechoic chamber. The measured patterns agree with the simulated patterns in gain, efficiency, and pattern shape (cf. Figs. 8 and 10). The measured patterns have a high level of orthogonality between the two ports in both the low and high bands of operation. The measured ECCs, calculated from the measured 3D patterns with uniform 3D APS, were below 0.1 in the low band and below 0.2 in the high band. The slightly higher measured ECC than the simulated ECC in the high band could be attributed to the practical feed structures. For example, when the 3D prototype model was re-simulated with the addition of 0.3 meters of cabling, microstrip lines, and SMA connectors, an average low band ECC of 0.14 and an average high band ECC of 0.25 were obtained. The average measured efficiency of both antennas in the low band (824 – 894 MHz) was -1.75dB. In the high band (1850 – 1990 MHz), the measured average total efficiencies were -1.2 dB and -1.7 dB for ports 1 and 2, respectively.

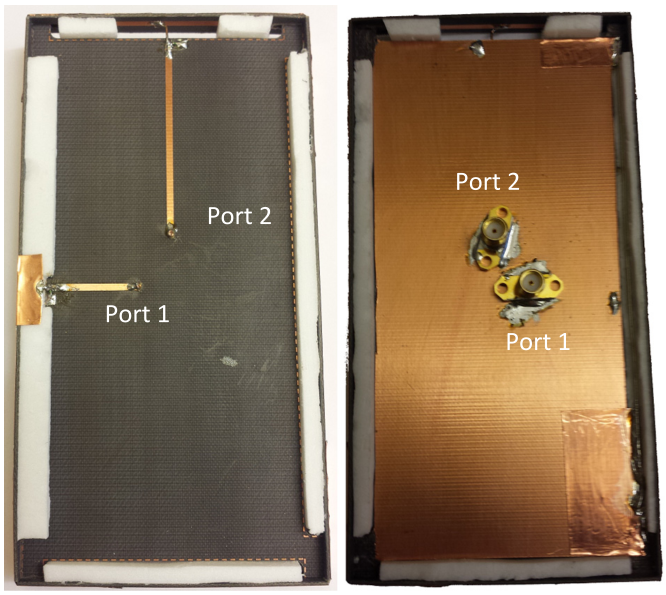

Fig. 9. Fabricated prototype of the multi-antenna multi-band bezel chassis.

VI. CONCLUSION

In this paper, the framework as described in [8] was used to design a multi-band multi-antenna bezel mobile phone chassis with low antenna correlation and sufficient bandwidth, for LTE operation. Through examining the characteristic currents and near-fields of the initial bezel structure, minor adjustments to the position and size of the ground plane were found that allowed simultaneous excitation of multiple characteristic modes at frequencies below 1 GHz. High frequency characteristic mode analysis provided insight into creating a slot antenna in the structure to support multiband operation at higher frequencies. The final structure was capable of supporting multiple efficient and uncorrelated antennas that can simultaneously cover LTE bands 2, 5, 6, 7, 15, 16, 19, and 25.

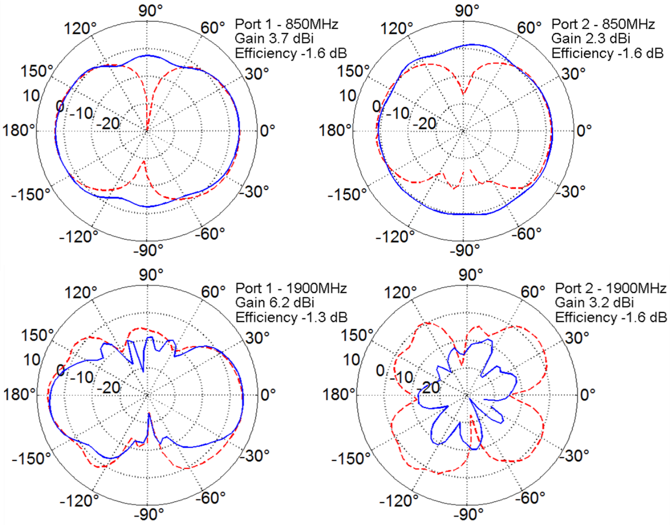

Fig. 10. Measured *y-z* (solid blue line) and *x-z* (dashed red line) principle plane patterns of port 1 and port 2.

REFERENCES

[1] B. K. Lau, “Multiple antenna terminals,” in *MIMO: From Theory to Implementation*, C. Oestges, A. Sibille, and A. Zanella, Eds. San Diego: Academic Press, 2011, pp. 267-298.

[2] R. F. Harrington and J. R. Mautz, "Computation of characteristic modes for conducting bodies," *IEEE Trans. Antennas Propag.,* vol. AP19, pp. 629-639, Sep. 1971.

[3] H. Li, Y. Tan, B. K. Lau, Z. Ying, and S. He, "Characteristic mode based tradeoff analysis of antenna-chassis interactions for multiple antenna terminals," *IEEE Trans. Antennas Propag.,* vol. 60, pp. 490-502, Feb. 2012.

[4] H. Li, B. K. Lau, Y. Tan, S. He, and Z. Ying, “Impact of current localization on the performance of compact MIMO antennas,” in *Proc. 5th Europ. Conf, Antennas Propag. (EuCAP’2011)*, Rome, Italy, Apr. 11-15, 2011, pp. 2423-2426.

[5] H. Li, B. K. Lau, Z. Ying, and S. He, "Decoupling of multiple antennas in terminals with chassis excitation using polarization diversity, angle diversity and current control," *IEEE Trans. Antennas Propag.,* vol. 60, pp. 5947-5957, 2012.

[6] H. Li, Z. Miers, and B. K. Lau, "Generating multiple characteristic modes below 1 GHz in small terminals for MIMO antenna design," in *Proc. IEEE Int. Symp. Antenna Propag.*, Orlando, FL, USA, Jul. 2013.

[7] H. Li, Z. Miers, and B. K. Lau, “Design of orthogonal MIMO handset antennas based on characteristic mode manipulation at frequency bands below 1 GHz,” *IEEE Trans. Antennas Propag.*, in press.

[8] Z. Miers, H. Li, and B. K. Lau, “Design of bandwidth enhanced and multiband MIMO antennas using characteristic modes,” *IEEE Antennas Wireless Propag. Lett.*, in press.

[9] Z. Miers, H. Li, and B. K. Lau, “Design of multi-antenna feeding for MIMO terminals based on characteristic modes,” in *Proc. IEEE Int. Symp. Antennas Propag*, Orlando, FL, Jul. 2013.